Active Contours Extension and Similarity Indicators for improved 3D Segmentation of Thyroid Ultrasound Images

P. Poudel[12], A. Illanes[2], C. Arens[2], C. Hansen[2] and M.Friebe[2]

[1]University of Bonn, [2]Otto-von-Guericke-University Magdeburg

ABSTRACT

Thyroid segmentation in tracked 2D ultrasound (US) using active contours has a low segmentation accuracy mainly due to the fact that smaller structures cannot be efficiently recognized and segmented. To address this issue, we propose a new similarity indicator with the main objective to provide information to the active contour algorithm concerning the regions that the active contour should continue to expand or should stop. First, a preprocessing step is carried out in order to attenuate the noise present in the US image and to increase its contrast, using histogram equalization and a median filter. In the second step, active contours are used to segment the thyroid in each 2D image of the dataset. After performing a first segmentation, two similarity indicators (ratio of mean square error, MSE and correlation between histograms) are computed at each contour point of the initial segmented thyroid between rectangles located inside and outside the obtained contour. A threshold is used on a final indicator computed from the other two indicators to find the probable regions for further segmentation using active contours. This process is repeated until no new segmentation region is identified. Finally, all the segmented thyroid images passed through a 3D reconstruction algorithm to obtain a 3D volume segmented thyroid. The results showed that including similarity indicators based on histogram equalization and MSE between inside and outside regions of the contour can help to segment difficult areas that active contours have problem to segment.

Keywords: Segmentation, Ultrasound Images, Thyroid Gland, 3D reconstruction, Active Contours without edges, Similarity Estimates

1. INTRODUCTION

Thyroid is one of the largest endocrine glands in human body. It is butterfly shaped gland located below the Adam's apple on the front of the neck. The thyroid is involved in several body mechanisms such as controlling energy sources usage, synthesis of proteins and controlling the body's sensitivity to hormones in other parts. Hence, it is very important to have a technique that allows the monitoring of the thyroid state over time. Most of the thyroid diseases like Graves' disease (excessive production of thyroid hormones), subacute thyroiditis (inflammation of thyroid), thyroid cancer, goiter (thyroid swelling), thyroid nodule (small abnormal lump grows in thyroid) [17, 18] involve changes in the shape and size of the thyroid. For this reason, it is essential to keep track of thyroid volume size over time. Ultrasound imaging is the modality of choice for the assessment. Volume determination can be achieved by manually observing the volume using three 2D thyroid images (one for each axis: x, y, z) and then applying an ellipsoidal formula or by volumetric ultrasonography [21]. The first technique is known to lack of accuracy and the second needs several minutes to be completed.

Several automatic approaches of 2D thyroid segmentation [2, 10, 13, 11, 14] as well as 3D one [3, 4, 6, 16] have been proposed. These methods use different approaches like image segmentation by edge detection, thresholding between different gray values, region splitting and merging, active contours without edges, localized region based active contour, distance regularized level sets, support vector machines (SVM), 3D deformable shapes, geodesic active contour level set formulation and neural networks approaches. These techniques have their own advantages as well as disadvantages but generally it is difficult to choose a threshold in inhomogeneous images when using thresholding method and with that produce a lot of false and discontinuous edges when using edge detection. All of these approaches use either 2D or 3D algorithm to segment the thyroid. With SVM and neural networks approaches, the segmentation is automatic, but they require a huge amount of data for network training.

We propose a new algorithm for thyroid segmentation that uses active contours as in [19] and add image similarity indicators to the automatic analysis in order to control the contour expansion. This approach was chosen as compared to segmentation in 3D because working with 2D images allows us to segment small structures in the image as well. The images have greater structural detail in the individual 2D images as compared to the image as a whole in 3D. In this way, individual 2D images are segmented and later reconstructed to produce a 3D segmented thyroid. We make use of active contours without edge algorithm developed by Chan-Vese [1] and region similarity indicators developed by our group to perform the segmentation in the ultrasound images. This approach result in more accurate 3D thyroid segmentation as compared to the method that only use active contours.

2. METHODS

This section presents the complete procedure used in this work, starting with the US acquisition data procedure, then continuing with the main part of this section corresponding to the 2D image segmentation algorithm and finally finishing with the reconstruction of the 3D segmented thyroid.

2.1 Ultrasound Data Acquisition

Fourteen healthy human subjects and seven thyroid phantoms were imaged using a LogicE9 ultrasound device (General Electric, USA) equipped with an electromagnetic tracking system. Each one of the 21 acquired US datasets involved more than 100 image slices, where each slice has been electromagnetically tracked resulting in a tracking matrix which gives the transformation from the tracking center to the center of the image slice. These tracking matrices are subsequently used for reconstructing the final segmented thyroid volume as presented in Section 2.3. Some examples of the thyroid images collected for one dataset are shown in Fig. 1. For comparison purposes, each slice of each dataset includes the manually segmented thyroid as ground truth performed by trained medical staff.

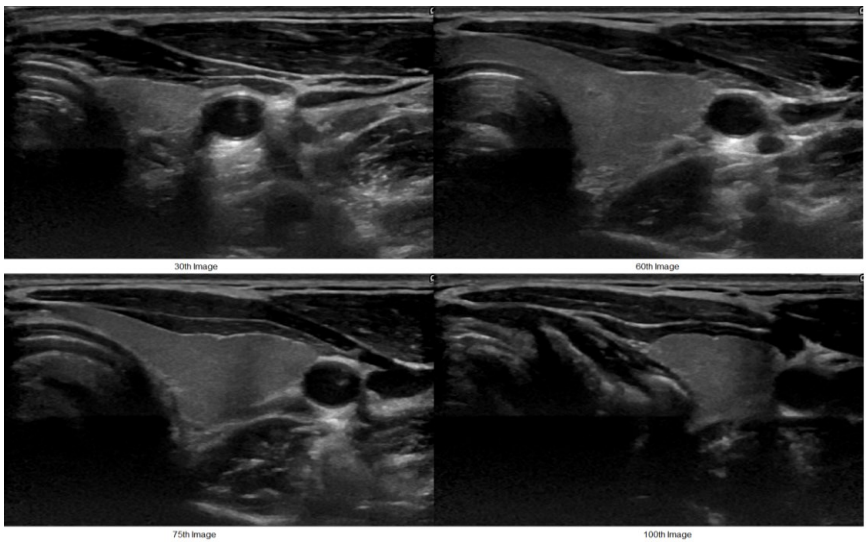

Fig. 1 Sample of thyroid images slices obtained during the data acquisition phase.

2.2 2D Image Segmentation Algorithm

The proposed algorithm takes the set of more than 100 acquired 2D image slices in one dataset and segments the tissue belonging to the thyroid in each one of the images. The algorithm interacts with the user only at the beginning of the procedure since it requires an initial mask for starting the active contour procedure. As shown in Fig. 2 the procedure for the segmentation of the full set of images is divided in five main steps: image preprocessing, initial mask location, active contour application, image similarity computation and the center of mass calculation.

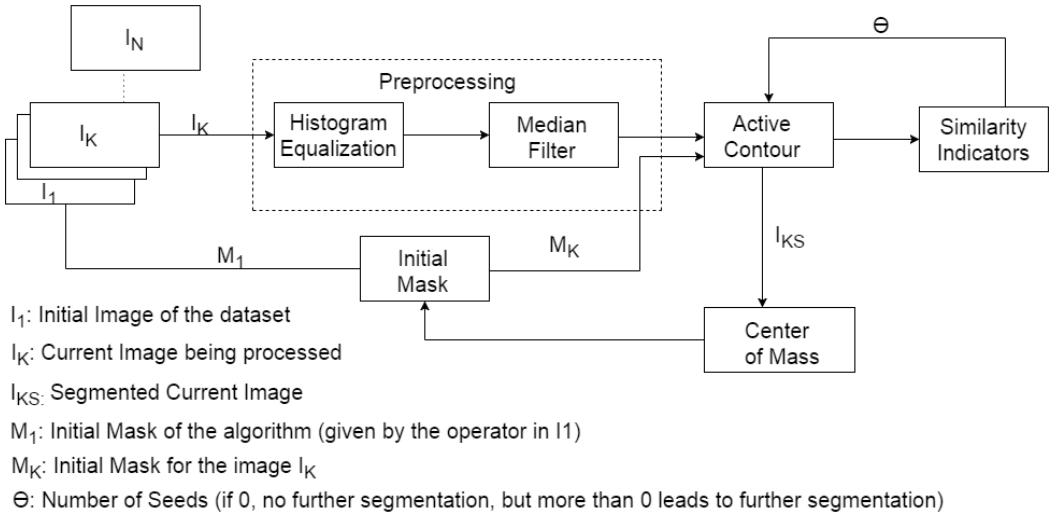

Fig. 2: Block Diagram of the 2D image segmentation procedure.

2.2.1 Image pre-processing

Ultrasound images usually have low contrast and also contain some noise like speckles (granular pattern) [6]. As ultrasound images are produced by the reflection of ultrasound waves from different body structures, the random fluctuations of these return signals produce the speckle noise [20]. Therefore a preprocessing step is required to enhance the contrast and attenuate the speckle noise. In this work the "histogram equalization technique" [7] is used for contrast enhancement as it helps to recover the lost contrast in the image by remapping the brightness values over all pixels. A median filter is then applied in order to attenuate the speckle noise and preserve edge information. The comparison between the thyroid image before and after pre-processing step is shown in Fig. 3.

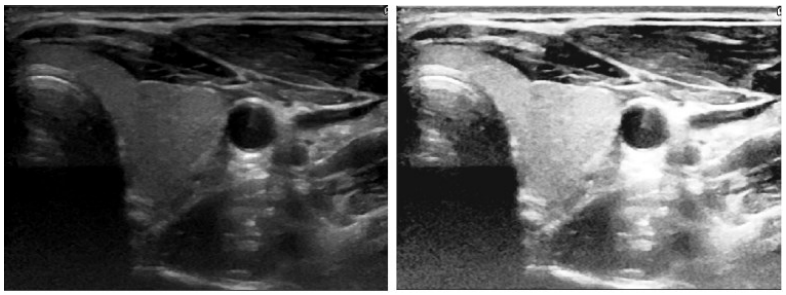

Fig. 3: Left: Thyroid US image before pre-processing, Right: Thyroid US image after pre-processing.

2.2.2 Initializing a mask for the active contour procedure

The Chan-Vese active contour without edges segmentation algorithm [1] used in this work starts with the definition of an initial mask with two regions: foreground (=1) and background (=0), that should be inside the thyroid (see Fig. 4). This is done because active contours techniques are sensitive to contour initialization. Wrong initialization of the mask can lead to segmentation of unnecessary structures in an image. The first initializing mask is given by the operator using the first image of the dataset to initialize the algorithm. The initializing mask of the rest of the images belonging to the dataset are automatically computed by the computation of a center of mass (see Section 2.3.4) of the already segmented image preceding the current one in process.

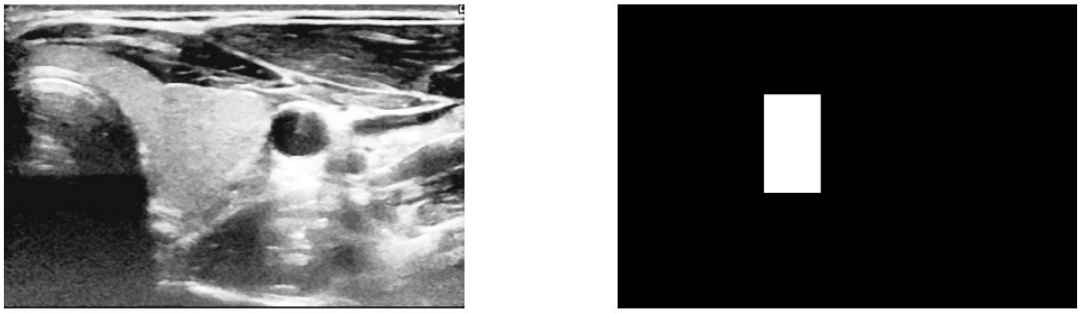

Fig. 4: Left: Thyroid US image after pre-processing, Right: Initial mask given by the operator for starting the segmentation procedure.

2.2.3 Active contour algorithm

The Chan-Vese active contour algorithm is mainly based on the minimization of the Mumford-Shah functional [6]. The evolution of the contour depends on different forces computed from the attributes of an image. In our case, we take the forces from the gradients and average intensity values.

Computing Signed Distance Function, SDF (Φ) from the mask
As active contour algorithm makes use of the level sets to keep track of evolving curve over time, SDF is computed to represent these level sets. Level sets are a framework used to analyse different surfaces and shapes that change over time, for example the splitting and merging of different shapes. SDF is computed from the initial mask by using the Euclidean distance. In level set formalism, the contour C is represented by the zero level set of Φ. Hence,

$$C = ((x, y), \Phi(x, y) = 0) \quad (1)$$

The goal is to evolve $\Phi(x, y)$ when the evolving contour (C) is the zero level set of $\Phi(x, y, t)$ at each time t.

Forces computation
The evolution of the initial mask is computed by making use of two different forces, from an image and from a curvature. The force from image controls the shrinking and expansion of the contour. It is computed by using the following equation.

$$F_{image} = \int_{insideC}(I - \mu_{in})^2 + \int_{outsideC}(I - \mu_{out})^2 \quad (2)$$

where I is the image, μ_{in} is the average inside the contour and μ_{out} is the average outside the contour.

In this equation, the first term tries to shrink the contour and the second term tries to expand the contour. These two forces get balanced when the contour reaches the boundary of the interested object. Similarly, a second force is computed to control the evolution of the contour and this force is termed as the force from the curvature. It is computed by using the kappa equation [8]. 8-neighbourhood points are taken into consideration when computing the force from curvature.

Contour evolution
The two forces calculated above are responsible for the evolution of the contour in each iteration. The evolution of the curve is approximated by using the Taylor expansion. The user can provide the number of iterations that the algorithm should run for. The algorithm stops after the given number of iterations are completed. This would be a parameter to be considered when a trade-off has to be considered between time and accuracy as more number of iterations might lead to over-segmentation and longer computation time. Similarly, very little iteration would result in under-segmentation and less computation time. To address these issues, we introduce the use of similarity indicators. The user can choose a smaller iteration number and the similarity indicators will control if further segmentation is required or not.

2.3.3 Region Similarity Indicator and Re-segmentation

Since some parts of the thyroid are very complex to segment in regions where gradient are not strong enough for active contour algorithms, we propose an additional post processing step in order to know which regions needs to expand further. For that, after the first segmentation is completed in an US image using the active contour algorithm, simple similarity indicators are computed at every contour point resulting from the initial segmentation. This similarity indicator is performed between two sub-images located inside and outside the contour at each contour position (see Fig. 5). For that, first of all two indicators are computed between the two contour point sub images. The first indicator (I_1) computes the mean square error (MSE) between the images and the second indicator (I_2) calculates the correlation between the histograms of both images. The final similarity indicators results from the division of both indicators $I_{similarity} = I_2/I_1$. A high value of this indicator is related with high similarity between regions, indicating that the contour can still expand on that region. In the other hand a low value indicates that the contour on that region should stop its expansion.

Finally, new initial masks are created automatically at each region where the indicator exceed an empirically chosen threshold. These masks will again undergo active contour algorithm to expand the segmented region. This process is repeated until no region presents similarities higher than the threshold.

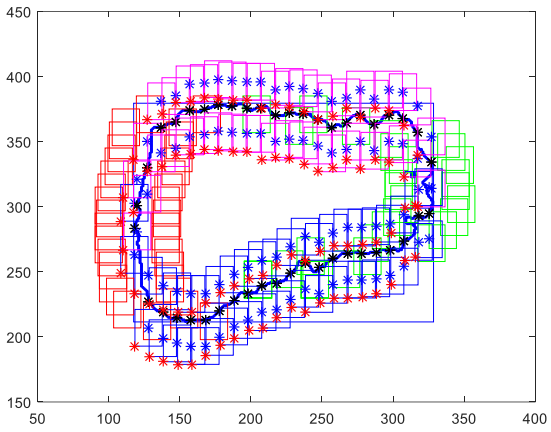

Fig. 5: Example of distribution of the sub images around the contour, which are used for computing similarity indicators.

2.3.4 Center of mass computation

Ones that in a given image slice the segmentation procedure has finished, it is necessary to compute automatically the initial mask for the next US image slice. For doing this the center of mass of the segmented thyroid is computed at the current image slice for being used as reference for the initialization mask of the next slice. The tracking matrices (see Section 2.1) can be used to find the center of each image. The angle and distance of the center of mass from the center of the preceding image is computed and these values are then used for determining the center location of initialization mask of the next image to be processed.

2.4 3D Reconstruction

The segmentation of all the images in the dataset produces a stack of segmented binary images. These images are then processed to create a video file. The video file along with the tracking data are then passed to a 3D reconstruction tool called Imfusion [5]. The reconstruction is done by the interpolation between corresponding images frames of the ultrasound sweep to fill the empty spaces.

3. RESULTS

In this section the main results obtained with the proposed algorithm are presented. First the main characteristics of the similarity algorithm results after a first segmentation is shown on one example of a thyroid US image. Then

different slices of the final segmentation result of the same dataset are shown, including also how the similarity algorithm performed after new expansions.

Fig. 6 shows the obtained indicators after a first segmentation, I_1 represent the MSE between the regions and I_2 representing the correlation between the histograms inside and outside the contour. Also we can observe the first segmentation contour and the comparison with the ground-truth and the final indicator after thresholding. Indicators I_1 and I_2 show inverse behavior and this is why the final indicator has been chosen as the division between both. As we see in the figure the final indicator has high values in the regions where the contour should continue to expand. This is evident when we look a 3D visualization of the final indicator.

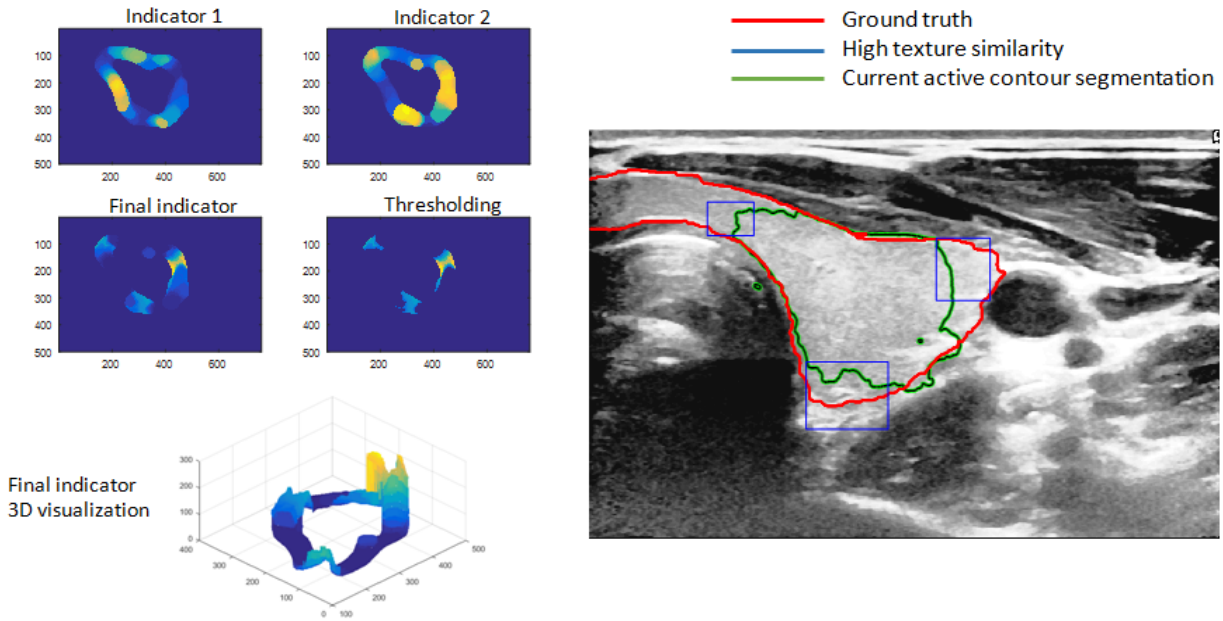

Fig. 6: Top Left: Indicators 1 shows the mean square of the pixel intensities between the two sub-images, Indicator 2 shows the ratio of correlation of between the histograms of the two sub-images, Result of using thresholding is shown in Final Indicator. Right: Visualization of new probable region of segmentation shown inside blue rectangles.

Fig. 7 shows the results in different slices when the active contour continues to expand after application of the similarity algorithm. It is possible to observe that, when we compare the results with the ground truth for the three slices, the highest values of the similarity function coincide with the regions where it is still possible to expand the active contour.

4. DISCUSSIONS AND CONCLUSIONS

The main objective of the presented work was to show preliminary results for improving active contour segmentation of 2D US thyroid images. Results shows that including similarity indicator based on histogram comparison and MSE between inside and outside regions of the contour can help for segmenting the difficult areas that active contours have problems to segment. To this similarity algorithm, other indicators can be added in the future to compare texture between regions, since texture is a very important issue on US thyroid images. Detailed result on all of our datasets will be available soon. One main drawback of this algorithm is that the computation time increases with every new segmentation detected by similarity indicators. One possibility for improving this problem is to perform multi-resolution analysis, i.e. one resolution for active contour expansion and another one for similarity computation.

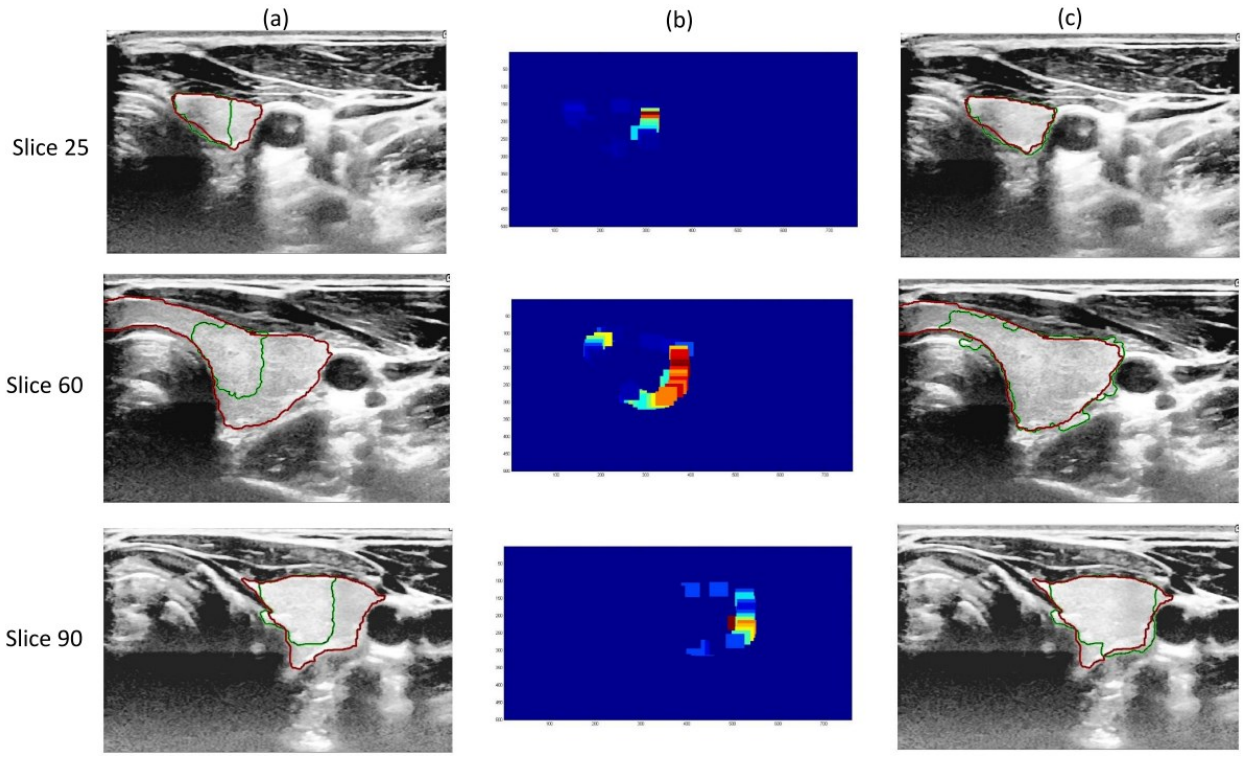

Fig. 7: Segmentation procedure for three slices belonging to the same dataset: (a) First active contour segmentation, (b) similarity indicator for the first performed segmentation, (c) final segmentation.

Acknowledgements

We thank General Electrics, USA for providing us with the financial support to carry out the research. Special thanks to our clinical partners at the University of Magdeburg, Piur Imaging GmbH, and the University Clinic in Jena (Prof. M. Freesmeyer) for helping to obtain the thyroid ultrasound datasets.

References

[1] Tony. F. Chan, Luminita A. Vese, "Active Contours Without Edges", IEEE Transactions on Image Processing, Vol. 10, No.2, February 2001.
[2] J. Zhao, W. Zheng, L. Zhang, H. Tian, "Segmentation of ultrasound images of thyroid nodule for assisting fine needle aspiration cytology".
[3] J. Dornheim, L. Dornheim, B. Preim, Klaus D. Tonnies, I. Hertel, G. Strauss, "Stable 3D Mass-Spring Models for the Segmentation of the Thyroid Cartilage".
[4] Eva N. K. Kollorz, Dieter A. Hahn, R. Linke, Tamme W. Goecke, J. Hornegger, T. Kuwert, "Quantification of Thyroid Volume Using 3-D Ultrasound Imaging", IEEE Transactions on Medical Imaging 27 (2008) No. 4 pp. 457-466.
[5] http://www.imfusion.de.
[6] C. Chang, Y. Lei, C. Tseng, S. Shih, "Thyroid Segmentation and Volume Estimation in Ultrasound Images", IEEE International Conference on Systems, Man and Cybernetics, 2008.
[7] Tay, P.C.,Garson, C.D., Acton, S.T., and Hossack, J.A., "Ultrasound Despeck-ling for Contrast Enhancement", IEEE Transactions on Image Processing, 2010, 19 (7), pp. 1847-1860.
[8] W. Aydi, N. Masmoudi, L. Kamoun, "Active Contour without Edges Vs GVF Active Contour for Accurate Pupil Segmentation", International Journal of Computer Applications(0975-8887) Vol. 54 - No.4, September 2012.
[9] R. Courant, K. Friedrichs, H. Lewy, "On the Partial Difference Equations of Mathematical Physics", IBM Journal,March 1967.

[10] J. Kaur and A. Jindal, “Comparison of thyroid segmentation algorithms in ultrasound and scintigraphy images.” International Journal of Computer Applications (0975-8887), 50(23), July 2012.
[11] D. Selvathi and V. S. Sharnitha, “Thyroid segmentation in ultrasound images using support vector machine”, International Journal of Neural Networks and Applications, 4(1):7–12, 2011.
[12] J. Zhao, W. Zheng, L. Zhang, and H. Tian, “Segmentation of ultrasound images of thyroid nodule for assisting fine needle aspiration cytology”.
[13] S. Agustin A and S. Suresh Babu, “Thyroid segmentation on us medical images: An overview”, International Journal of Emerging Technology and Advanced Engineering, 2(2), December 2012.
[14] Nasrul H. Mahmood and Akmal H. Rusli, “Segmentation and area measurement for thyroid ultrasound image”, International Journal of Scientific and Engineering Research, 2, December 2011.
[15] C. Y. Chang, Y. F. Lei, C. H. Tseng, and S. R. Shih, “Thyroid segmentation and volume estimation in ultrasound images”, IEEE International Conference on Systems, Man and Cybernetics, 2008.
[16] A. Osman, “Automated evaluation of three dimensional ultrasound datasets.” 2013.
[17] Understanding thyroid problems - the basics, “http://www.webmd.com/women/guide/understanding-thyroid-problems-basics”.
[18] Image collection: Human anatomy, “http://www.webmd.com/women/picture-of-the-thyroid”.
[19] P. Poudel, C. Hansen, J. Sprung and M. Friebe, “3D Segmentation of Thyroid Ultrasound Images using Active Contours”, IEEE EMBS, August 2016.
[20] R. Gir, L. Jain, and R. Rai, “Speckle reduction of synthetic aperture radar images using median filter and savitzky-golay filter”, International Journal of Computer Applications, 113(11), March 2015.
[21] R. Malago, M. D’Onofrio, M. Ferdeghini, W. Mantovani, C. Colato, P. Brazzarola, M. Motton, R. Mucelli, “Thyroid volumetric quantification: comparative evaluation between conventional and volumetric ultrasonography”, J Ultrasound Med 2008 Dec, 27(12) 1727-33.